Materials Science and Engineering B 187 (2014) 21–25

Contents lists available at ScienceDirect

Materials Science and Engineering B

journal homepage: www.elsevier.com/locate/mseb

Short communication

Electrophoretic deposition of ZnO nanostructures: Au nanoclusters on Si substrates induce self-assembled nanowire growth

Claudia Sandoval[a], Oscar Marin[b], Silvina Real[a], David Comedi[b], Mónica Tirado[a,*]

[a] Laboratorio de Nanomateriales y Propiedades Dieléctricas, Facultad de Ciencias Exactas y Tecnología, Universidad Nacional de Tucumán, San Miguel de Tucumán, Argentina
[b] CONICET – LAFISO, Facultad de Ciencias Exactas y Tecnología, Universidad Nacional de Tucumán, San Miguel de Tucumán, Argentina

ARTICLE INFO

Article history:
Received 26 December 2013
Received in revised form 31 March 2014
Accepted 13 April 2014
Available online 28 April 2014

Keywords:
ZnO nanowires
Electrophoretic deposition
Photoluminescence

ABSTRACT

The present work reports the self-assembled growth of ZnO nanowires on silicon substrate with nanometer sized Au clusters using electrophoretic deposition technique at room temperature without a sacrificial template. A colloidal suspension of ≈5 nm sized ZnO nanoparticles dispersed in 2-propanol was used (nanoparticle bandgap of 3.47 eV as determined from absorbance measurements). The results show that the Au nanoclusters on the silicon substrate induce the self-assembly of the ZnO nanoparticles into vertically aligned ZnO nanowires. This effect is tentatively explained as being due to increased electric field intensities near the Au nanoclusters during the electrophoretic deposition. Photoluminescence measurements reveal the presence of quantum confined excitons and a relatively low concentration of deep defects in the nanowires. The electric field guided growth of semiconductor nanostructures at room temperature has great industrial potential as it minimizes production costs and enables the use of substrate materials not withstanding high temperatures.

1. Introduction

The growth of ZnO nanowire (ZnO NW) arrays has been studied extensively due to their many potential applications such as sensor technology [1], memory devices [2], optoelectronics [3], flexible transparent electronics and photovoltaic devices [4]. The great interest regarding ZnO nanostructures arises due to the large surface-to-volume ratio [1], optical transparency [5], tunable optoelectronic properties [6,7], high exciton binding energy and isoelectronic point, piezoelectricity and other properties. Some methods of ZnO NW growth include carbon thermal reduction [8], chemical vapor deposition and vapor transport deposition [9]. These growth techniques involve high temperature processes, which result in high production costs and a severe limitation on the type of growth substrates. Therefore, the implementation of growth techniques at low temperature is very desirable. In this sense, methods based on hydrothermal synthesis at room [10,11] and moderately larger temperatures [12,13] have been reported. However, these methods have often limitations for industrial scale use due to the large reaction times involved and the difficult control of growth as a result of the large number of parameters affecting the synthesis (pH, precursor concentrations, temperature, mixing time, pressure).

In recent years, the strengths of electrophoretic deposition (EPD) technique for the growth of nanostructured materials have been recognized [14]. Advantages of EPD include the possibility of performing it at room temperature [15] and of depositing the material of interest on almost any substrate; the requirement of very simple and low cost equipment and its easy scalability up to large dimensions. All these confer EPD great technological and industrial interest [14].

In EPD, the deposition on the electrode occurs via assembling of charged particles dispersed in a colloidal suspension, which migrate by the action of a suitable electric field [16]. The characteristics of materials deposited via EPD are influenced by parameters of the colloidal suspension as well as physical parameters related to the deposition (electric field, electrode nature, deposition time) [14].

For the growth of NWs, sacrificial templates such as porous alumina have been traditionally used. This has been an important drawback for the general application of EPD given that templates are expensive and provide physical limits on the resulting NW aspect ratios and diameters that can be achieved by this technique.

In this communication, we show that Au nano-clusters, which can be easily pre-deposited onto the growth electrode by simple

* Corresponding author. Tel.: +54 93814123181; fax: +54 381 436 4157.
E-mail addresses: mtirado@herrera.unt.edu.ar, tiradomonica@yahoo.com (M. Tirado).

http://dx.doi.org/10.1016/j.mseb.2014.04.002
0921-5107/

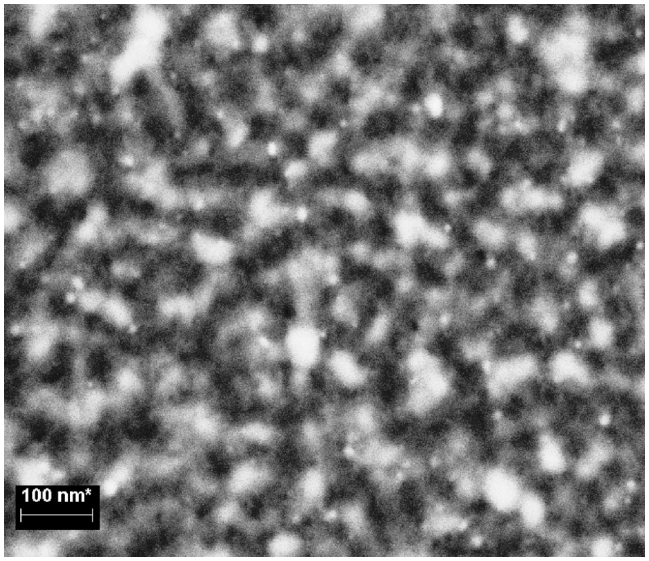

Fig. 1. SEM micrograph of Au-modified silicon surface used for ZnO deposition. The size of Au nanoclusters obtained was between 15 and 25 nm.

physical vapor deposition, can be used to promote vertically aligned NW growth in EPD.

2. Experimental procedure

ZnO nanoparticle (NP) colloidal suspensions were prepared for EPD following the method reported by Bahnemann et al. [17]. Two solutions of $Zn(C_2H_5O)_2{\cdot}2H_2O$ (Anedra ACS reagent grade) and NaOH (Anedra ACS reagent grade) in 2-propanol (Merck ACS reagent grade 99.5%) with concentrations of 1.2×10^{-3} M and 2×10^{-2} M, respectively, were used in order to obtain transparent suspensions of ZnO NPs. The chemical properties of the resultant colloidal suspension, such as conductivity, viscosity, density, pH and zeta potential, were measured using a Metler Toledo conductivity meter model MC 226, an Anton Paar model Stabinger viscometer, a Metler Toledo model MA235, and a Malvern Nano Zeta Sizer model Zen3600, respectively. All measurements were carried out at $T = 22\,^{\circ}C$.

Absorbance and fluorescence (325 and 350 nm excitation wavelengths) spectra were recorded from colloidal solutions held within a 1 cm length quartz cell using a Varian Cary 50 UV/Visible spectrophotometer, and a Shimadzu 160A UV/Visible spectrofluorometer, respectively.

ZnO NP sizes were measured on scanning electron microscopy (SEM) images of ZnO NPs deposited on silicon substrate by the drop-coating technique. Sizes were also estimated from the absorbance measurements on the NP colloidal suspensions.

The acrylic EPD cell design allows use of one electrode as the growth substrate for deposition of ZnO nanostructures and a parallel high purity Pt sheet as the counter electrode. The substrates used were Si (1 0 0) wafer cuts with a 500 nm thick thermally grown SiO_2. Au nanoclusters were deposited on some of the substrates by thermally evaporating an Au film with nominal "thickness" of 3 nm, and then promoting film dewetting and clustering by heating the substrates to 500 °C for 30 min. During the process a steady H_2 flow was established and the pressure was kept constant at 100 mTorr [18,19]. This procedure resulted in Au nanocluster with sizes ranging between 15 and 25 nm, as shown in Fig. 1.

Prior to EPD, the ZnO NP colloidal suspension was always sonicated for 10 min (Branson 200 sonicator) to disperse the NPs. The resulting nanostructures were studied by SEM and energy-dispersive X-ray spectroscopy (EDX) to determine their morphology and composition, respectively. Photoluminescence measurements were performed with a HeCd laser (Kimmon IK5452R-E) operating at 325 nm excitation wavelength and a CCD spectrometer (Avantes AVASPEC-ULS-USB2).

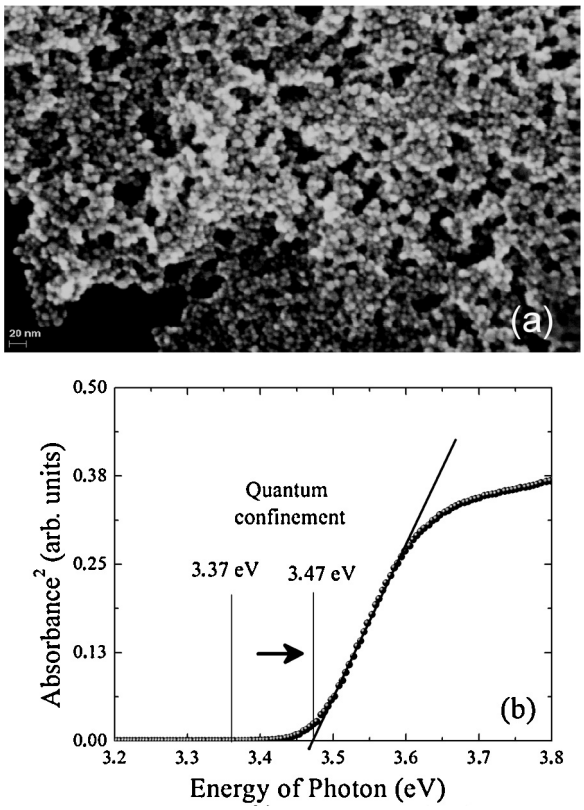

Fig. 2. (a) SEM micrograph of ZnO nanoparticles used for electrophoretic deposition. (b) Absorption spectra of ZnO nanoparticles in solution. An E_g value of 3.47 eV was estimated from absorption spectra.

3. Results and discussion

Fig. 2(a) shows a SEM micrograph of ZnO NPs that result after depositing a drop of the colloidal suspension on a Si substrate and the evaporation of the 2-propanol solvent. The ZnO NPs obtained exhibit uniform shape and a narrow size distribution around 5 nm diameter. The bandgap (E_g) of ZnO NPs was determined from the absorbance spectra using the linear method [17]. The energy was calculated by extrapolating the best linear fit to the linear region in a $(Abs \times h\upsilon)^2$ vs. $h\upsilon$ plot [20]. The E_g value thus obtained was ~3.47 eV, as shown in Fig. 2(b) [21]. This value is in agreement with other E_g values reported for ZnO NPs for the same size [22]. The E_g for ZnO bulk is 3.35 eV; the quantum confinement effect is responsible for the bandgap blueshift in ZnO NPs.

The chemical properties of the colloidal suspension were: conductivity = 3.03 μS/cm, density = 0.7889 g/cm^3, viscosity = 2.2466 mPa s, pH = 9.098 and zeta potential ~20 mV. Due to the positive values of the zeta potential, cathodic EPD was always performed.

Fig. 3 shows SEM micrographs of the ZnO film grown on silicon substrate without Au nanoclusters. The applied voltage, the electrode distance and deposit time were 40 V, 7 mm and 1 h, respectively. Due to the high resistivity of the silicon substrate used as electrode, a large deposition time was needed for a complete coating with ZnO NPs [14]. As shown in the Fig. 3(a), although a complete coating of the silicon substrate was achieved, the deposited film was not really homogeneous and showed several

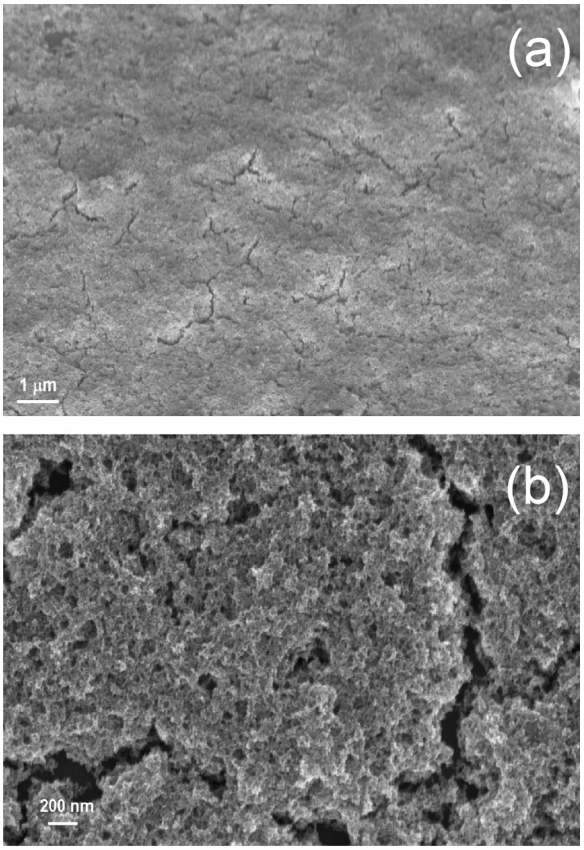

Fig. 3. (a) SEM micrograph of ZnO film deposited electrophoretically on silicon electrode. The applied voltage, electrode distance and deposition time were 40 V, 7 mm and 1 h respectively. (b) Same as (a), but with higher magnification to show the underlying nanoporous structure.

cracks. A higher magnification revealed a nanoporous structure (Fig. 3(b)), which is a possible consequence of a low packing factor typical of colloidal suspensions of NPs [23]. Stappers et al. studied the effect of suspension conductivity on the morphology of films obtained by EPD, suggesting that low conductivity suspensions result in non-uniform films in the nanoscale, due to the almost constant driving force for particle deposition [24]. The high resistivity of the silicon substrate used and the low conductivity of the colloidal suspension are the responsible for the heterogeneity in the nanoscale of films obtained [25].

The modified silicon electrodes with Au nanoclusters induced a columnar packing of ZnO NPs. As a result, ZnO nanowires were obtained instead of a nanoporous ZnO film (compare Fig. 4(a) with Fig. 3). For this deposition, the applied voltage, electrode distance and time deposition were 30 V, 7 mm and 1 h, respectively. The obtained sample showed a large density of ZnO nanowires, with a preferential vertical orientation. The diameters of ZnO nanowires obtained ranged between 20 and 90 nm and the lengths were around ~1.2 μm.

Au nanoclusters (15–25 nm) change the morphology of the working electrode and hence may promote concentration of the electric field lines on nanoclusters inducing the deposition of particles preferentially on them. This effect is due to the metallic character of the nanoclusters, which implies the vanishing of the electric field tangential components at the nanoclusters surfaces [26]. As a result of this boundary condition, electric field lines will align normally to the nanocluster surfaces, producing the deviation of the electric field lines away from the uncovered Si substrate and their "focusing" on the Au nanoclusters [27]. Since the ZnO nanoparticles are electrophoretically transferred from the colloidal suspension to the working electrode along the electric field lines, they will tend to accumulate on the nano metallic clusters, thus explaining ZnO nanowire formation on the Au-nanocluster modified Si electrode.

In addition, the narrow ZnO NP size distribution is expected to favor their ordered packing on the substrate thus favoring NW formation [25]. As seen from Fig. 4(b), thin nanowires seem to grow first, then merging together to form thicker nanowires. This

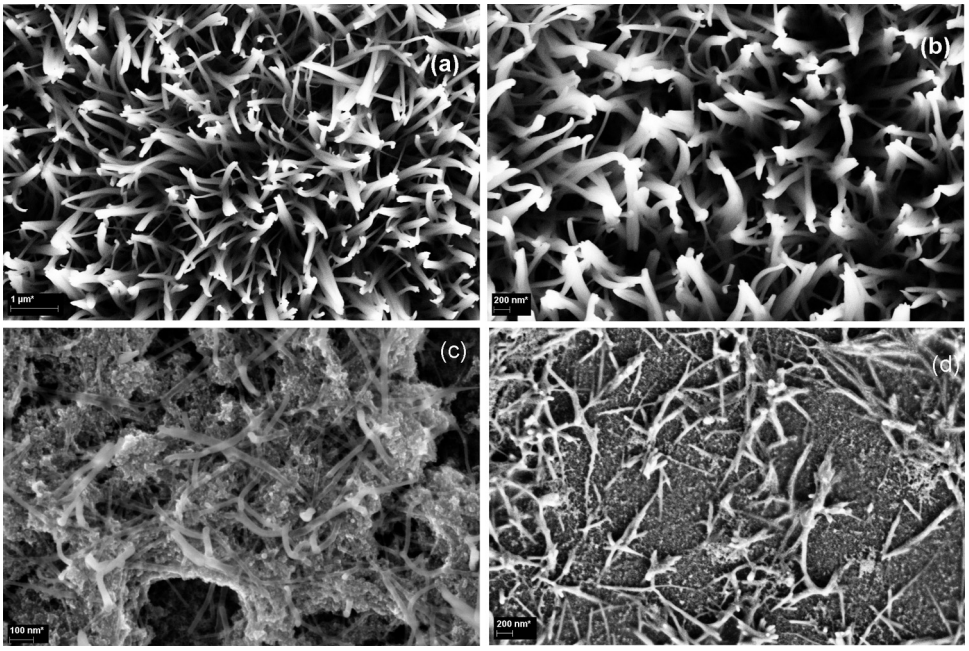

Fig. 4. SEM micrograph of ZnO nanostructures deposited electrophoretically on gold-modified silicon substrates. (a,b) ZnO oriented nanowires obtained with an applied voltage of 30 V. (c) ZnO nanoporous film/non-oriented nanowires obtained with an applied voltage of 20 V. (d) Non-oriented ZnO nanowires obtained with an applied voltage of 40 V. The electrode distance and deposition time were 7 mm and 1 h, respectively, for all samples.

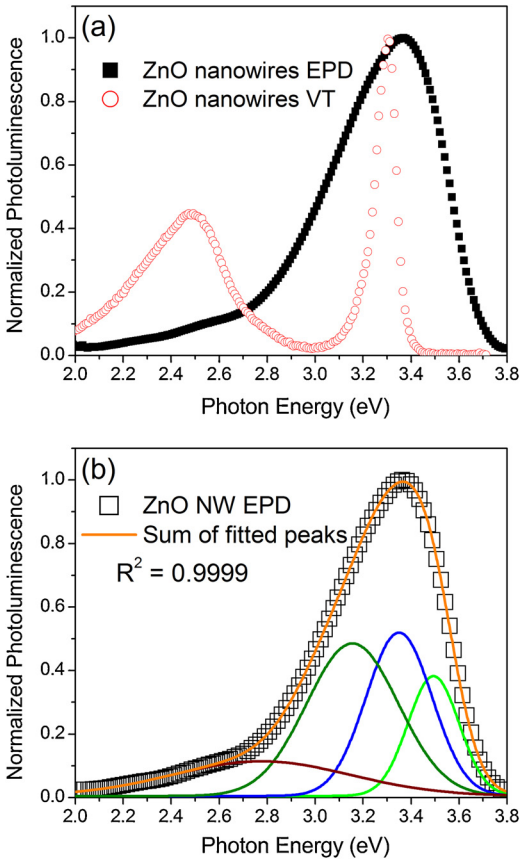

Fig. 5. (a) Normalized photoluminescence spectrum from ZnO nanowires grown by vapor transport technique (empty circles) and electrophoretic deposition technique (black squares). (b) Multigaussian fit of the photoluminescence spectrum corresponding to ZnO nanowires grown by EPD. (For interpretation of the references to color in this figure legend, the reader is referred to the web version of the article.)

morphology confers a large surface area to samples fabricated by this method, which represents high technological potential, for example for applications in biochemical sensors where the selective sensing of molecules of biological interest, such as DNA [1], can be performed after proper functionalization of the vertically aligned ZnO NWs. In addition, applications of ZnO nanostructures in vapor or gas sensors has been demonstrated for several analytes, such as ethanol, NO_2, NH_3, CO and O_2 [11,28].

Fig. 4(c) and (d) shows SEM images of additional ZnO deposits on Au nanocluster covered Si substrates obtained for applied voltages of 20 and 40 V, respectively. As observed, for 20 V a nanoporous ZnO layer with embedded non-oriented ZnO nanowires is obtained, while for 40 V only non-oriented nanowire growth occurs. The electrophoretic velocity is proportional to the applied electric field (applied voltage/separation between the electrodes) which affects deposition rate and the quality of deposition morphology [29]. If the applied voltage is high, the nanoparticles move so fast that they cannot find enough time to place themselves in the best position to form a close-packed structure [14].

Fig. 5(a) shows a PL spectrum for the ZnO nanowires shown in Fig. 4(a). A corresponding PL spectrum for ZnO nanowires (~80 nm diameter) obtained by a vapor transport (VT) technique [30] is shown for comparison purposes. Both spectra are normalized to yield one at their maxima. For the ZnO nanowires grown by EPD, the green emission intensity is lower and a broad peak is observed in the UV-blue region (peak center at 3.37 eV). This is in contrast to the VT ZnO NWs, which exhibit a narrow UV peak and a pronounced green emission. Fig. 5(b) shows a multigaussian fit to the EPD ZnO NW PL spectrum. As observed, the experimental PL is well reproduced with 4 Gaussian components centered at 2.77, 3.15, 3.35 and 3.49 eV. A fit with three peaks was also tested however it was found to be unsatisfactory. The emission at 3.35 eV corresponds to the well-know excitonic transitions in bulk ZnO. The emission at 3.49 eV corresponds to blueshifted excitonic transitions in very thin (few nm thick) ZnO NWs where quantum confinement is important. Theory calculations have shown that interstitial Zn (Zn_i) leads to shallow defect states located at 0.22 eV below the conduction band [31,32] and hence this defect is a candidate to explain the emission at 3.15 eV. Probably, the presence of Zn_i centers in EPD NWs is caused by incomplete zinc acetate reactions during the synthesis of nanoparticles. The green emission (~2.77 eV), in turn, has been commonly associated with recombination processes involving oxygen vacancies or surface defects [33,34]. Hence, the low green emission from the EPD ZnO NW samples indicates relatively low oxygen vacancy and/or surface defect concentrations [7].

4. Conclusions

The self-assembled EPD growth of vertically oriented ZnO NWs from a colloidal suspension of ZnO NPs in 2-propanol has been achieved at room temperature without the use of sacrificial templates. The self-assembled growth is shown to be promoted by the presence of pre-deposited Au nanoclusters on Si substrates. The PL spectrum for the NWs obtained shows a broad UV-blue excitonic emission peak tentatively interpreted as being due to contributions from quantum confinement and transitions involving shallow defects.

The results presented here expand the applications of the EPD technique for deposition of nanostructured materials. The growth of semiconductors NWs at room temperature has a great industrial interest because it minimizes the production costs compared with conventional growth techniques and enables the use of substrates sensitive to high temperature treatments.

Acknowledgments

This work was supported by FONCyT (PICT 2010-0400) and CIUNT 26/E419. We are grateful to Dr. Néstor E. Katz and Lic. Juan H. Mecchia Ortiz (INQUINOA-CONICET, Instituto de Química Física, FBQyF, UNT) for assistance with fluorescence and absorbance measurements on the ZnO NP suspensions.

References

[1] R. Niepelt, U.C. Schröder, J. Sommerfeld, I. Slowik, B. Rudolph, R. Möller, B. Saise, A. Csaki, W. Fritzche, C. Ronnig, Nanoscale Res. Lett. 6 (2011) 511.
[2] Y. Chiang, W. Chang, C. Ho, C. Chen, C. Ho, S. Lin, T. Wu, J. He, IEEE Trans. Electron Devices 58 (2011) 1735.
[3] M.T. Chen, M.P. Lu, Y.J. Wu, J. Song, C.Y. Lee, M.Y. Lu, Y.C. Chang, L.J. Chou, Z.L. Wang, L.J. Chen, Nano Lett. 10 (2010) 4387.
[4] H.E. Unalan, P. Hiralal, D. Kuo, B. Parekh, G. Amaratunga, M. Chhowalla, J. Mater. Chem. 18 (2008) 5909.
[5] S. Ju, A. Facchetti, Y. Xuan, J. Liu, F. Ishikawa, P. Ye, C. Zhou, T.J. Marks, D.B. Janes, Nat. Nanotechnol. 2 (2007) 378.
[6] K.F. Lin, H.M. Cheng, H.C. Hsu, L.J. Lin, W.F. Hsieh, Chem. Phys. Lett. 409 (2005) 208.
[7] T.J. Athauda, P. Hari, R.R. Ozer, ACS Appl. Mater. Interfaces 5 (2013) 6237.
[8] N. Qin, X. Wang, Q. Xiang, J. Xu, Sens. Actuators B: Chem. 191 (2014) 770.
[9] D.P. Singh, Sci. Adv. Mater. 2 (2010) 245.
[10] D. Bao, P. Gao, L. Wang, Y. Wang, Y. Chen, G. Chen, G. Li, C. Chang, W. Qin, Chempluschem 78 (2013) 1266.
[11] S. Wei, S. Wang, Y. Zhang, M. Zhou, Sens. Actuators B: Chem. 192 (2014) 480.
[12] P. Gao, L. Wang, Y. Wang, Y. Chen, X. Wang, G. Zhang, Chem. Eur. J. 18 (2012) 4681.
[13] H. Men, P. Gao, B. Zhou, Y. Chen, C. Zhu, G. Xiao, L. Wang, M. Zhang, Chem. Commun. 46 (2010) 7581.
[14] L. Besra, M. Liu, Prog. Mater. Sci. 52 (2007) 1.
[15] X. Yin, X. Liu, L. Wang, B. Liu, Electrochem. Commun. 12 (2010) 1241.
[16] P. Lommens, D. Van Thourhout, P.F. Smet, D. Poelman, Z. Hens, Nanotechnology 19 (2008) 245301.

[17] D.W. Bahnemann, C. Kormann, M.R. Hoffmann, J. Phys. Chem. 91 (1987) 3789.
[18] R.S. Wagner, W.C. Ellis, Appl. Phys. Lett. 4 (1964) 89.
[19] N.C. Vega, M. Tirado, D. Comedi, A. Rodriguez, T. Rodriguez, G.M. Hughes, C.R.M. Grovenor, F. Audebert, Mater. Res. 16 (2013) 597.
[20] J. Pankove, Optical Processes in Semiconductors, Prentice-Hall, Englewood Cliffs. N.J, 1971.
[21] L.E. Brus, J. Chem. Phys. 80 (1984) 9.
[22] R. Viswanatha, S. Sapra, B. Satpati, P.V. Satyam, B.N. Dev, D.D. Sarma, J. Mater. Chem. 14 (2004) 661.
[23] C. Ji, I.P. Shapiro, P. Xiao, J. Eur. Ceram. Soc. 29 (2010) 3167.
[24] L. Stappers, L. Zhang, O. Van der Biest, J. Fransaer, J. Colloid Interface Sci. 328 (2008) 436.
[25] R. Moreno, B. Ferrari, in: J.H. Dickerson, A.R. Boccaccini (Eds.), Electrophoretic Deposition of Nanomaterials, Chapter 2, Springer, New York, USA, 2012, pp. 73–128.
[26] J.D. Jackson, Classical Electrodynamics, John Wiley & Sons, Inc., New York, USA, 1962.
[27] C. Grosse, M. Tirado, IEEE Trans. Educ. 39 (1996) 69.
[28] Z. Fan, J.G. Lu, IEEE Trans. Nanotechnol. 5/4 (2006) 393.
[29] P.J. Sides, C.L. Wirth, C. Prieve, in: J.H. Dickerson, A.R. Boccaccini (Eds.), Electrophoretic Deposition of Nanomaterials, Chapter 1, Springer, New York, USA, 2012, p. 24.
[30] N.C. Vega, R. Wallar, J. Caram, G. Grinblat, M. Tirado, R.R. LaPierre, D. Comedi, Nanotechnology 23 (2012) 275602.
[31] C.H. Ahn, Y.Y. Kim, D.C. Kim, S.K. Mohanta, H.K. Cho, J. Appl. Phys. 105 (2009) 013502.
[32] N.H. Alvi, K. Ul Hasan, O. Nur, M. Willander, Nanoscale Res. Lett. 6 (2011) 130.
[33] Z. Ibupoto, K. Khun, M. Eriksson, M. AlSalhi, M. Atif, A. Ansari, M. Willander, Materials 6 (2013) 3584.
[34] A.B. Djurisicí, Y.H. Leung, K.H. Tam, L. Ding, W.K. Ge, H.Y. Chen, S. Gwo, Appl. Phys. Lett. 88 (2006) 103107.